

Bridging Perception and Reasoning: Token Reweighting for RLVR in Multimodal LLMs

Jinda Lu¹ Junkang Wu¹ Jinghan Li¹ Kexin Huang¹ Shuo Yang²
Guoyin Wang³ Jiancan Wu¹ Xiang Wang¹ Xiangnan He¹

Abstract

Extending Reinforcement Learning with Verifiable Rewards (RLVR) to multimodal large language models (MLLMs) faces a fundamental challenge: their responses inherently interleave **perception-related tokens**, which ground visual content, with **reasoning-related tokens**, which construct reasoning chains. These token types instantiate distinct yet interdependent capacities — *visual grounding and symbolic reasoning* — making isolated optimization insufficient. Through token-level empirical analysis, we demonstrate that optimizing either perception- or reasoning-only tokens consistently underperforms full optimization, underscoring their inherent coupling. To address this, we propose a *plug-and-play* **Token-Reweighting (ToR)** strategy that explicitly models this interdependence by identifying critical tokens of both types and dynamically reweighting them during RLVR training. Applied on top of existing methods (*e.g.*, GRPO and DAPO), ToR delivers consistent performance gains across multiple multi-modal reasoning benchmarks, achieving state-of-the-art performance with both accurate visual grounding and coherent reasoning.

1. Introduction

Reinforcement Learning with Verifiable Rewards (RLVR) has substantially advanced the reasoning ability of large language models (LLMs) on complex tasks (Lambert et al., 2025; Shao et al., 2024; Guo et al., 2025; Yang et al., 2025a). Extending RLVR to multimodal large language models (MLLMs), however, is non-trivial: generated responses *interleave* tokens that ground visual content (**perception**) with tokens that drive symbolic inference (**reasoning**), as illustrated in Figure 1. Existing MLLM RLVR variants typically

¹University of Science and Technology of China ²Peking University ³Independent Researcher. Contact at: Jinda Lu <lujd@mail.ustc.edu.cn>.

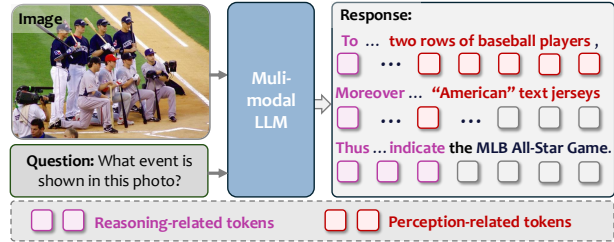


Figure 1. MLLM responses typically involve two types of critical tokens: (1) reasoning-related tokens to construct reasoning chains, and (2) perception-related tokens to ground visual content.

optimize these capabilities in isolation — either via chain-of-thought objectives for reasoning (Huang et al., 2025; Wei et al., 2025) or perception-oriented augmentations for perception (Wang et al., 2025e; Xiao et al., 2025; Liu et al., 2025a) — leaving their interaction underexplored.

We hypothesize that this separated optimization is suboptimal because perception and reasoning are fundamentally interdependent at the token level. To empirically validate this claim, we conduct a controlled “selective optimization” study under Group Relative Policy Optimization (GRPO) (Shao et al., 2024). We identify reasoning-related tokens via high **next-token entropy** (following recent insights on reasoning forks (Wang et al., 2025c; Cheng et al., 2025)), and perception-related tokens via **visual sensitivity**, measured as the change in token log-probability when conditioning on the image versus a text-only context (details in Section 3). We then train models while masking gradients on non-selected tokens, comparing three settings: optimizing only reasoning-related tokens, only perception-related tokens, and all tokens (vanilla GRPO).

Across selection ratios (20%, 30%, 50%), optimizing only reasoning tokens underperforms vanilla GRPO (*e.g.*, $\sim 2\%$ absolute drop on we-math benchmark), and optimizing only perception tokens fares worse (*e.g.*, $\sim 3\%$ drop, with 20% and 30% tokens even worse than the baseline model); neither matches training on all tokens (Figure 2). Qualitatively, reasoning-only models produce coherent-looking chains of thought yet misinterpret key visual content, while perception-only models preserve low-level grounding but fail to integrate it into coherent reasoning. These results sup-

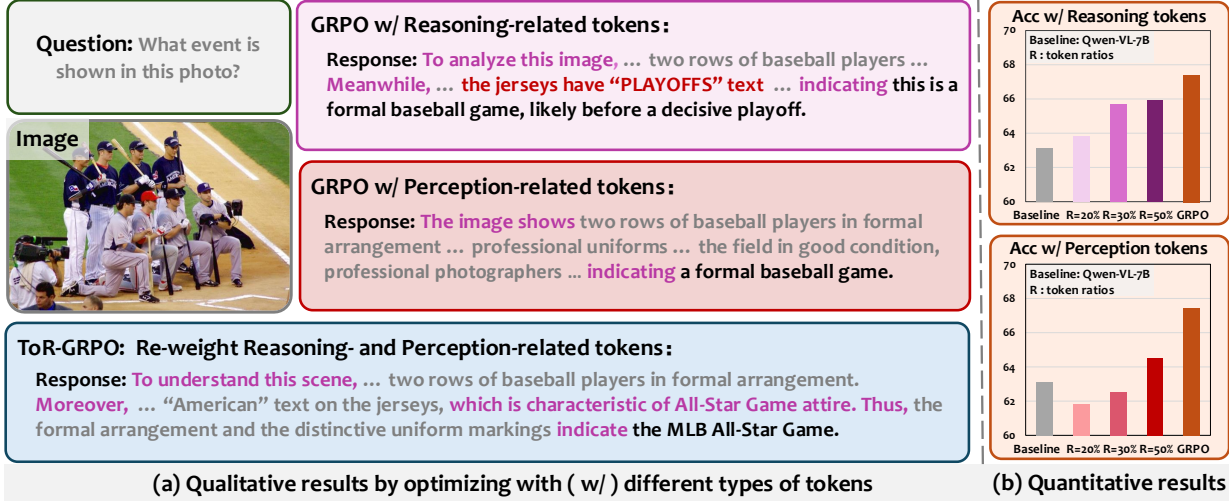


Figure 2. Performance comparison over the wemath benchmark (Qiao et al., 2024) when optimizing different token types with GRPO (Shao et al., 2024). Results across selection ratios 20%, 30%, or 50% show that optimizing either reasoning-only or perception-only tokens underperforms all tokens. Qualitative examples are selected from the best-performing checkpoints.

port our hypothesis: *perception and reasoning are coupled capabilities that demand joint optimization.*

Building on this insight, we propose **Token-Reweighting (ToR)**, a lightweight, plug-and-play module for RLVR that jointly optimizes perception and reasoning. Instead of treating all tokens equally or optimizing subsets in isolation, ToR strategically identifies the most critical perception- and reasoning-related tokens and adaptively reweights their importance in the policy gradient calculation. This mechanism explicitly models their interdependence, encouraging the MLLM to integrate visual grounding into its logical deliberations. As shown in Figure 2, applying ToR to GRPO (**ToR-GRPO**) not only recovers the performance lost from selective optimization but surpasses the standard GRPO baseline, confirming our effectiveness.

In summary, we show that perception and reasoning in MLLMs are tightly coupled at the token level and should be optimized jointly. By explicitly reweighting perception- and reasoning-related tokens during training, Token Reweight- ing enables MLLMs to improve reasoning decisions while preserving accurate visual grounding, resulting in consistent gains across various models and benchmarks.

2. Preliminaries

In this section, we revisit Reinforcement Learning with Verifiable Rewards (RLVR) procedure and representative RLVR optimization strategies for Multi-modal Large Language Models (MLLMs).

2.1. Reinforcement Learning with Verifiable Rewards

Reinforcement Learning with Verifiable Rewards (RLVR) enhances multi-modal large language models (MLLMs) by aligning model outputs with verifiable answers. Given a multi-modal input with ground truth from a batch of B samples, $(I^b, q^b) \in \{I^b, q^b\}_{b=1}^B$, and $y^b \in \{y^b\}_{b=1}^B$, where I^b , q^b , and y^b denotes the image, question, and ground-truth respectively, the model π_θ generates output σ^b containing a reasoning process and a prediction. The prediction is enclosed in `\boxed{.}` while reasoning is delimited by `<think>...</think>`, enabling automated verification against the ground truth answers. RLVR employs a binary reward function $\mathbf{R}(\cdot)$ to determine whether the answer is correct by comparing the model output σ^b with ground truth y^b . The goal of RLVR is to maximize the reward function, formalized as:

$$\mathcal{J}_{\text{RLVR}}(\theta) = \max_{\theta} \mathbb{E}_{\{(I^b, q^b) | y^b\}_{b=1}^B} \mathbb{E}_{\sigma^b \sim \pi_\theta(\cdot | I^b, q^b)} [\mathbf{R}(\sigma^b, y^b)]. \quad (1)$$

2.2. RLVR Optimization Algorithms

Group Relative Policy Optimization (GRPO). As a widely adopted RLVR optimization strategy, GRPO stabilizes training by computing advantages within response groups (Shao et al., 2024). Concretely, given a batch of samples $\{(I^b, q^b) | y^b\}_{b=1}^B$, the GRPO objective is:

$$\mathcal{J}_{\text{GRPO}}(\theta) = \mathbb{E}_{\substack{q \sim P(Q) \\ \{o_i\} \sim \pi_{\theta_{\text{old}}}} \left(\frac{1}{G} \sum_{i=1}^G \frac{1}{|o_i|} \sum_{t=1}^{|o_i|} \min \left(\frac{\pi_\theta(o_{i,t})}{\pi_{\theta_{\text{old}}}(o_{i,t})} \hat{A}_{i,t}, \right. \right. \\ \left. \left. \text{clip} \left(\frac{\pi_\theta(o_{i,t})}{\pi_{\theta_{\text{old}}}(o_{i,t})}, 1 \pm \epsilon \right) \hat{A}_{i,t} \right) - \beta \cdot \mathbb{D}_{KL}(\pi_\theta \| \pi_{\text{ref}}) \right), \quad (2)$$

where G is the rollout group size for each input, and the clip function restricts the importance ratio within $[1 - \epsilon, 1 + \epsilon]$.

Moreover, the advantage can be formulated as:

$$\begin{cases} \hat{A}_{i,t}^b = \frac{\mathbf{R}_i^b - \text{mean}(\mathbf{R}^b)}{\text{std}(\mathbf{R}^b)}, \\ \mathbf{R}_i^b = \mathbb{I}(\text{is_equivalent}(o_i^b, y^b)), \end{cases} \quad (3)$$

where $\mathbb{I}(\cdot)$ is the indicator function, $\text{is_equivalent}(\cdot)$ extracts the predictions from the model output o_i^b and compares with the ground truth y^b .

Decoupled Clip and Dynamic Sampling Policy Optimization (DAPO). DAPO (Yu et al., 2025b) improves upon GRPO by removing KL regularization and introducing clip-higher, dynamic sampling, and token-level loss from the GRPO loss, achieving new state-of-the-art performance. Specifically, the DAPO objective for the batch of samples $\{(I^b, q^b) \mid y^b\}_{b=1}^B$ can be formalized as:

$$\mathcal{J}_{\text{DAPO}}(\theta) = \mathbb{E}_{\substack{q \sim P(Q) \\ \{o_i\} \sim \pi_{\theta_{\text{old}}}}} \left[\frac{1}{\sum |o_i|} \sum_{i=1}^G \sum_{t=1}^{|o_i|} \min \left(\frac{\pi_{\theta}(o_{i,t})}{\pi_{\theta_{\text{old}}}(o_{i,t})} \hat{A}_{i,t}, \text{clip} \left(\frac{\pi_{\theta}(o_{i,t})}{\pi_{\theta_{\text{old}}}(o_{i,t})}, 1 - \epsilon_{\text{low}}, 1 + \epsilon_{\text{high}} \right) \hat{A}_{i,t} \right) \right], \quad (4)$$

where ϵ_{low} and ϵ_{high} decouple the clipping thresholds for negative and positive advantages, respectively. In this work, we apply our token-reweighting strategy to both GRPO and DAPO, demonstrating its general applicability across various RLVR optimization strategies.

3. Approach

In this section, we introduce **Token Reweighting (ToR)**, a simple strategy that jointly optimizes reasoning- and perception-related tokens for reinforcement learning. We first describe how to identify these two types of critical tokens, and then present how ToR integrates them into existing RLVR objectives such as GRPO and DAPO.

3.1. Token Identification

Multimodal reasoning responses interleave tokens that serve distinct functional roles. Some tokens correspond to critical reasoning decisions, while others primarily ground the response in visual inputs. We therefore identify two complementary token types—*reasoning-related* and *perception-related* tokens—using the intrinsic model signals.

3.1.1. REASONING-RELATED TOKENS

Identification. Recent studies (Wang et al., 2025c; Cheng et al., 2025) have shown that tokens with high predictive entropy often correspond to pivotal “forking” points in reasoning chains, reflecting the model’s decision uncertainty. Motivated by this observation, we identify reasoning-related tokens based on token-level entropy during rollout generation. Given the i -th generated response $\mathbf{o}_i^b =$

$\{o_{i,1}^b, o_{i,2}^b, \dots, o_{i,L_i}^b\}$ conditioned on the image I^b , and then question q^b from the input batch $\{(I^b, q^b)\}_{b=1}^B$, the prediction entropy at position t is computed as:

$$H_{i,t}^b = - \sum_{v \in \mathcal{V}_{\text{top-}p}} P_{\theta}(o_{i,t}^b = v \mid \mathbf{o}_{i,<t}^b, I^b, q^b) \cdot \log P_{\theta}(o_{i,t}^b = v \mid \mathbf{o}_{i,<t}^b, I^b, q_i^b), \quad (5)$$

where $\mathcal{V}_{\text{top-}p}$ denotes the set of vocabulary tokens within the top- p cumulative probability ($p = 0.95$). This top- p truncation avoids the influence of extremely low-probability tokens and is consistent with the rollout sampling process.

To aggregate across the rollout batch, we collect all token entropies into a set:

$$\mathcal{H} = \{H_{i,t}^b \mid b = 1, \dots, B; i = 1, \dots, G; t = 1, \dots, L_i^b\}. \quad (6)$$

The reasoning-token set is then defined by selecting the top- α_r fraction of tokens with the highest entropy across the batch:

$$\mathcal{T}_r = \{(b, i, t) \mid H_{i,t}^b \geq \text{Percentile}_{1-\alpha_r}(\mathcal{H})\}, \quad (7)$$

where α_r controls the fraction of selected tokens. Intuitively, these high-uncertainty positions correspond to pivotal points where reasoning chains are shaped.

Influences of reasoning-related tokens. Restricting optimization to the reasoning-token set \mathcal{T}_r concentrates gradient updates on high-entropy decision points, thereby reducing reasoning uncertainty, as illustrated in Figure 3(a). However, excluding perception-related tokens weakens visual grounding, allowing perception errors to persist during training. As a result, reasoning-only optimization sharpens local decision confidence but fails to support robust multimodal reasoning, leading to inferior performance compared to full-token GRPO.

3.1.2. PERCEPTION-RELATED TOKENS

Identification of perception-related tokens. While reasoning-related tokens capture decision uncertainty, perception-related tokens highlight positions whose predictions strongly depend on visual inputs. To quantify this dependence, we compare the token log-probabilities under two conditions: (i) *with image*, conditioned on both I^b and q^b ; and (ii) *without image*, where the image channel is replaced by an empty placeholder \emptyset and the model is conditioned only on q^b .

Given the i -th generated response $\mathbf{o}_i^b = \{o_{i,1}^b, \dots, o_{i,T_i}^b\}$, the visual-sensitivity score at position t is computed as:

$$S_{i,t}^b = |\log \pi_{\theta}(o_{i,t}^b \mid \mathbf{o}_{i,<t}^b, I_i^b, q_i^b) - \log \pi_{\theta}(o_{i,t}^b \mid \mathbf{o}_{i,<t}^b, \emptyset, q_i^b)|, \quad (8)$$

where $\pi_{\theta}(o_t \mid \cdot)$ is the token-level policy. A large $S_{i,t}$ indicates a strong visual influence on token $o_{i,t}$. Aggregating across the rollout batch, the perception-token set is

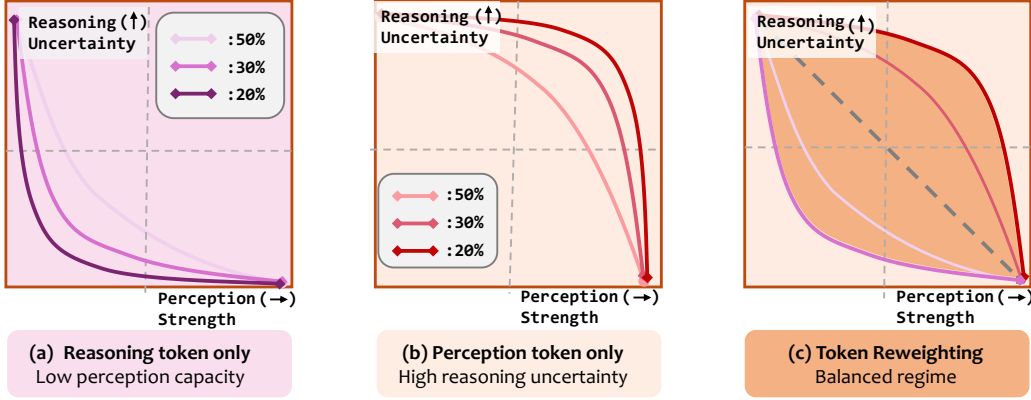


Figure 3. Comparison of perception strength and reasoning uncertainty under different token ratios during GRPO optimization. (a) Reasoning-token-only optimization suffers from limited perception capacity. (b) Perception-token-only optimization is sensitive to high reasoning uncertainty. (c) Token reweighting yields a balanced regime by adaptively trading off perception strength and reasoning uncertainty, where the shaded region indicates effective optimization outcomes. Dashed lines denote the balance where increased perception strength compensates for reasoning uncertainty.

defined as the top- α_p fraction of tokens with the highest visual-sensitivity:

$$S = \{S_{i,t}^b \mid b = 1, \dots, B; i = 1, \dots, G; t = 1, \dots, L_i^b\} \quad (9)$$

$$\mathcal{T}_p = \{(b, i, t) \mid S_{i,t}^b \geq \text{Percentile}_{1-\alpha_p}(S)\},$$

where α_p controls the selection ratio. This batch-level percentile selection ensures consistent token selection thresholds across rollout batches.

Influences of perception-related tokens. Restricting optimization to the perception-token set \mathcal{T}_p concentrates gradient updates on visually sensitive positions, thereby strengthening visual grounding, as conceptually illustrated in Figure 3(b). However, excluding reasoning-related tokens prevents effective optimization of high-uncertainty decision points, leaving reasoning ambiguity unresolved. As a result, perception-only optimization preserves low-level visual fidelity but fails to support coherent reasoning, leading to inferior performance compared to full-token GRPO.

3.2. Token Reweighting

As conceptually illustrated in Figure 3, optimizing only reasoning-related or perception-related tokens leads to imbalanced optimization. Reasoning-only optimization reduces uncertainty but lacks visual grounding, while perception-only optimization improves grounding without resolving high-uncertainty reasoning decisions.

Motivated by this observation, we introduce *Token Reweighting* (ToR), a unified framework that jointly incorporates reasoning- and perception-critical tokens. Instead of masking gradients to a single token subset, ToR assigns token-specific weights during policy optimization, enabling simultaneous reduction of reasoning uncertainty and strengthen-

ing of visual grounding. In this way, ToR explicitly models the interdependence between reasoning and perception at the token level.

Specifically, for the given input batch $\{(I^b, q^b)\}_{b=1}^B$, we constructed the reasoning-related token set \mathcal{T}_r and the perception-related token set \mathcal{T}_p , and thus the GRPO objective with token reweighting (**ToR-GRPO**) is:

$$\mathcal{J}_{\text{ToR-GRPO}}(\theta) = \mathbb{E}_{\{(I^b, q^b)\}_{b=1}^B} \mathbb{E}_{\{o_i^b\}_{i=1}^G \sim \pi_{\theta_{\text{old}}}} \left\{ \frac{1}{G} \sum_{i=1}^G \frac{1}{|o_i^b|} \sum_{t=1}^{|o_i^b|} \left[\gamma_r \cdot \mathbb{I}[(b, i, t) \in \mathcal{T}_r] + \gamma_p \cdot \mathbb{I}[(b, i, t) \in \mathcal{T}_p] \right] \cdot \min \left[r_{\theta}(o_{i,t}^b) \hat{A}_{i,t}^b, \text{clip}(r_{\theta}(o_{i,t}^b), 1 - \epsilon, 1 + \epsilon) \hat{A}_{i,t}^b \right] - \beta \mathbb{D}_{KL}[\pi_{\theta} \parallel \pi_{\text{ref}}] \right\} \quad (10)$$

Similarly, the DAPO objective with the token-weighting strategy (**ToR-DAPO**) is:

$$\mathcal{J}_{\text{ToR-DAPO}}(\theta) = \mathbb{E}_{\{(I^b, q^b)\}_{b=1}^B} \mathbb{E}_{\{o_i^b\}_{i=1}^G \sim \pi_{\theta_{\text{old}}}} \left\{ \frac{1}{\sum_{i=1}^G |o_i^b|} \sum_{i=1}^G \sum_{t=1}^{|o_i^b|} \left[\gamma_r \cdot \mathbb{I}[(b, i, t) \in \mathcal{T}_r] + \gamma_p \cdot \mathbb{I}[(b, i, t) \in \mathcal{T}_p] \right] \cdot \min \left[r_{\theta}(o_{i,t}^b) \hat{A}_{i,t}^b, \text{clip}(r_{\theta}(o_{i,t}^b), 1 - \epsilon_{\text{low}}, 1 + \epsilon_{\text{high}}) \hat{A}_{i,t}^b \right] \right\}. \quad (11)$$

$r_{\theta}(o_{i,t}^b)$ is the importance sampling ratio, formalized as:

$$r_{\theta}(o_{i,t}^b) = \frac{\pi_{\theta}(o_{i,t}^b \mid I_i^b, q_i^b, o_{i,<t}^b)}{\pi_{\theta_{\text{old}}}(o_{i,t}^b \mid I_i^b, q_i^b, o_{i,<t}^b)}. \quad (12)$$

Here, γ_r weights reasoning-related tokens, emphasizing critical decision points in reasoning chains; γ_p weights perception-related tokens, emphasizing the integration of visual context. Tokens outside these sets are excluded from

optimization (*i.e.*, assigned a weight of zero for advantage calculation). This reweighting ensures gradients focus on tokens essential for both reasoning and perception, improving both training efficiency and effectiveness.

Discussion Compared with existing approaches, ToR offers several key advantages: **1 Plug-and-play.** A simple reweighting mask integrates seamlessly into standard RLVR objectives, without introducing extra pipeline modifications. **2 Self-contained.** Critical tokens are identified purely from the model’s intrinsic uncertainty and visual sensitivity, eliminating the need for external priors. **3 Joint optimization.** By explicitly modeling the interdependence between reasoning and perception tokens, ToR enables balanced and simultaneous enhancement of both capabilities.

4. Experiment

In this section, we elaborate on the effectiveness of our token reweighting strategy. Specifically, we first introduce the details of our experimental settings. Next, we present the ablation studies, and finally, we compare our results with those of state-of-the-art methods across various benchmarks.

4.1. Experimental Settings

We adopt the Geometry3K (Lu et al., 2021) dataset for training and validation, following existing methods (Liu et al., 2025a; Xiao et al., 2025), which consists of 2,100 training samples and 300 validation samples. Moreover, we employ the multi-modal framework EasyR1 (Yaowei et al., 2025) for reinforcement learning training, and following the works in (Liu et al., 2025a) for evaluation. Evaluation is conducted with five benchmarks, including four for visual reasoning: MathVerse (Zhang et al., 2024), MathVision (Wang et al., 2024), MathVista (Lu et al., 2024b), and WeMath (Qiao et al., 2024), and one for visual perception: HalluBench (Guan et al., 2024).

Implementation details. We adopt Qwen2.5-VL-7B (Bai et al., 2025) as our baseline model by following existing works in (Meng et al., 2025; Liu et al., 2025a). Specifically, all experiments are conducted using 8 NVIDIA H800 GPUs (80 GB memory for each), with the default settings in EasyR1: a learning rate of $1e^{-6}$, a global batch size of 128, a rollout batch size of 512, a rollout n as 12.

4.2. Ablation Studies

We conduct ablation studies to analyze how different token-level optimization strategies affect multimodal reasoning performance. In particular, we focus on understanding whether reasoning-related or perception-related tokens can be optimized in isolation, and whether jointly reweighting both types of tokens is necessary for robust learning. All ablation experiments are conducted using Qwen-2.5-VL-7B

Table 1. Performance comparison with different ratios of reasoning-related tokens (α_r). We vary the proportion of reasoning-related tokens from 20% to 80%.

α_r	HalluBench	MathVerse	WeMath	MathVision	MathVista
20%	62.8	49.3	63.9	26.5	69.2
30%	65.1	<u>50.7</u>	65.6	<u>27.0</u>	<u>70.0</u>
40%	66.1	50.1	65.9	26.3	69.4
50%	67.1	50.4	66.0	<u>27.0</u>	68.7
60%	67.1	50.0	67.1	27.3	70.3
70%	<u>67.5</u>	50.8	<u>67.3</u>	26.7	<u>70.0</u>
80%	68.4	50.3	67.6	26.8	69.0
GRPO	69.8	50.8	67.4	27.3	70.5

Table 2. Performance comparison with different ratios of perception-related tokens (α_p). We vary the proportion of perception-related tokens from 20% to 80%.

α_p	HalluBench	MathVerse	WeMath	MathVision	MathVista
20%	65.9	38.6	61.4	22.7	65.5
30%	69.3	44.9	64.8	24.5	67.8
40%	67.8	44.7	<u>65.9</u>	25.1	67.4
50%	<u>68.3</u>	39.5	62.9	27.6	<u>68.7</u>
60%	68.1	<u>45.1</u>	65.8	25.0	67.4
70%	65.1	45.8	66.8	25.2	68.9
80%	53.4	<u>45.1</u>	65.8	<u>25.9</u>	68.1
GRPO	69.8	50.8	67.4	27.3	70.5

with GRPO on the Geometry3K training set, and evaluated on HalluBench, WeMath, MathVerse, MathVision, and MathVista.

Failure of isolated token optimization. We first investigate whether selectively optimizing a single token type is sufficient for multimodal reasoning. Specifically, we isolate reasoning-related tokens or perception-related tokens according to our token identification criteria, vary their proportions, and mask gradients on all remaining tokens.

Table 1 reports results when varying the proportion of reasoning-related tokens (α_r). Across all benchmarks, selectively optimizing reasoning tokens consistently underperforms full-token GRPO. Notably, even on reasoning-intensive benchmarks such as WeMath and MathVerse, reasoning-only optimization fails to match the performance of full-token training. This indicates that effective reasoning optimization critically depends on perception-related context, and that reasoning signals alone are insufficient to guide robust policy learning in multimodal settings.

Table 2 shows the results of perception-only optimization by varying the proportion of perception-related tokens (α_p). While perception-only reweighting achieves competitive performance on perception-oriented benchmarks such as HalluBench, it leads to substantial degradation on reasoning-demanding tasks, particularly on MathVerse and WeMath. These results highlight a complementary failure mode: perception signals alone cannot be effectively utilized without concurrent reasoning supervision.

Table 3. Performance under different combinations of reasoning and perception tokens. We vary the perception-related weight from 0.1 to 1.5 while keeping the reasoning-related weight fixed at 1.0.

γ_p	HalluBench	MathVerse	WeMath	MathVision	MathVista
0.1	66.5	50.8	65.5	27.3	69.7
0.3	69.1	<u>52.1</u>	67.4	28.6	70.8
0.5	<u>71.3</u>	53.0	68.7	<u>28.3</u>	71.9
0.7	70.5	51.1	<u>68.1</u>	27.5	70.8
0.9	72.2	50.9	67.0	27.2	<u>71.4</u>
1.1	<u>71.3</u>	49.9	67.3	26.9	69.3
1.3	70.2	49.9	<u>68.1</u>	26.5	68.9
1.5	69.4	49.6	66.2	26.8	68.7
GRPO	69.8	50.8	67.4	27.3	70.5

Together, these results demonstrate that optimizing either reasoning-related or perception-related tokens in isolation is insufficient for robust multimodal reasoning. Although both token types are individually important, their learning dynamics are tightly coupled during optimization.

Joint reweighting of reasoning and perception tokens.

Motivated by the above failure modes, we next investigate whether jointly reweighting reasoning- and perception-related tokens can alleviate the limitations of isolated optimization. Table 3 reports results when fixing the weight of reasoning-related tokens to 1.0 and varying the weight of perception-related tokens (γ_p).

We observe that jointly reweighting both token types consistently improves performance over isolated optimization across all benchmarks. In particular, moderate perception token weights lead to improved reasoning performance while preserving strong perception accuracy. In contrast, extremely low or high perception token weights degrade performance, indicating that over-emphasizing either token type disrupts the balance of effective multimodal reasoning.

Overall, a perception token weight of $\gamma_p = 0.5$ provides a strong and stable trade-off across benchmarks, and we adopt this setting as the default configuration in subsequent experiments. Regarding the token selection ratio, we find that increasing the proportion of selected tokens generally improves performance, but also gradually approaches full-token optimization, diminishing the effect of selective reweighting. Lower ratios, while not optimal, still yield competitive performance without destabilizing training. We therefore adopt 30% as a conservative operating point that provides sufficient learning signal while preserving the benefits of selective token reweighting. Importantly, our method does not rely on precise tuning of this ratio, and similar qualitative trends are observed under nearby settings.

Discussion on overlapping tokens. During early stages of GRPO training on Geometry3K, approximately 12% of tokens are identified as both reasoning- and perception-related. As training progresses, this overlap ratio evolves dynamically. Empirically, we observe that while perfor-

mance degrades when either token type is optimized in isolation, the degradation is consistently smaller when retaining reasoning-related supervision. Therefore, for overlapping tokens, we assign them the same weight as reasoning-related tokens during reweighting, which yields more stable optimization behavior in practice.

4.3. Comparison with state-of-the-art approaches

We compare our token re-weighting strategy with a broad set of state-of-the-art multi-modal LLMs, including open-source instruction-tuned models (e.g., InternVL-2.5 (Chen et al., 2024), InternVL-3 (Zhu et al., 2025), LLaVA-OneVision (Li et al., 2025a), and Qwen-2.5-VL-7B (Bai et al., 2025)) and recent reinforcement learning with verifiable reward (RLVR) approaches (e.g., R1-VL (Zhang et al., 2025a), Vision-R1 (Huang et al., 2025), R1-OneVision (Yang et al., 2025b), OpenVLThinker (Deng et al., 2025b), MM-Eureka (Meng et al., 2025), ThinkLite (Wang et al., 2025d), VLAA-Thinker (Chen et al., 2025a), and NoisyRollout (Liu et al., 2025a)). Results are summarized in Table 4.

- **Comparison with RLVR baselines.** Under the same training data scale (2.1K Geo3K samples), ToR consistently improves strong RLVR baselines. Applying token reweighting to GRPO improves MathVerse from 50.8 to 53.0 and HalluBench from 69.8 to 72.4. Similarly, ToR-DAPO outperforms DAPO across all benchmarks, with particularly notable gains on WeMath and MathVista.

- **Generalization across data and model scales.** ToR continues to provide consistent improvements when scaling the training data from Geo3K to ViRL-39K, achieving the strongest overall performance on Qwen-2.5-VL-7B across all benchmarks. Moreover, ToR generalizes to a smaller Qwen-2.5-VL-3B backbone, consistently improving over the DAPO baseline despite reduced model capacity.

Overall, Table 4 shows that token re-weighting demonstrates robust and generalizable improvements to RLVR-based multimodal learning, yielding consistent gains across model sizes, training data scales, and diverse reasoning and perception benchmarks. Importantly, all ToR results are obtained using the same hyperparameter settings across different model backbones and data scales.

5. Related Work

In this section, we first briefly summarize recent advances in computer vision (Lu et al., 2025a; 2023; 2025b; 2024a), especially those that focus on enhancing reasoning capabilities in Multi-modal LLMs, and then, we illustrate related methods for reinforcement learning with verifiable rewards. Finally, we enumerate the differences between our approach and related methods.

Table 4. Performance comparison of multi-modal LLMs under different model and data scales. Following existing works (Liu et al., 2025a; Xiao et al., 2025), we highlight the data size with blue and red for SFT and RL, respectively. The best value in each column is shown in **bold**, and the second-best is underlined.

Model	Data Size	MathVerse	MathVision	MathVista	WeMath	HalluBench
<i>Open-source Models</i>						
InternVL-2.5-8B (Chen et al., 2024)	-	39.5	19.7	64.4	-	67.3
InternVL-3-8B (Zhu et al., 2025)	-	39.5	29.3	71.6	37.1	-
LLaVA-OneVision-7B (Li et al., 2025a)	-	26.2	-	63.2	-	48.4
Qwen2.5-VL-7B-Instruct (Bai et al., 2025)	-	46.2	25.0	67.5	63.1	64.6
<i>RLVR on Qwen-2.5-VL-7B</i>						
R1-VL-7B (Zhang et al., 2025a)	260K+10K	40.0	24.7	63.5	-	-
Vision-R1-7B (Huang et al., 2025)	200K+10K	52.4	-	<u>73.5</u>	-	-
R1-OneVision-7B (Yang et al., 2025b)	155K+10K	46.1	22.5	63.9	62.1	65.6
OpenVLThinker-7B (Deng et al., 2025b)	35K+15K	48.0	25.0	71.5	67.8	70.8
MM-Eureka-Qwen-7B (Meng et al., 2025)	15K	50.5	28.3	71.5	65.5	68.3
ThinkLite-7B-VL (Wang et al., 2025d)	11K	50.2	27.6	72.7	69.2	71.0
VLAA-Thinker-7B (Chen et al., 2025a)	25K	49.9	26.9	68.8	67.9	68.6
NoisyRollout-7B (Liu et al., 2025a)	2.1K	53.2	28.5	72.6	69.6	72.1
GRPO (Shao et al., 2024)	2.1K (Geo3K)	50.8	27.3	70.5	67.4	69.8
ToR-GRPO	2.1K (Geo3K)	53.0	28.6	71.9	68.9	<u>72.4</u>
DAPO (Yu et al., 2025b)	2.1K (Geo3K)	50.6	26.5	70.3	69.3	67.9
ToR-DAPO	2.1K (Geo3K)	53.4	<u>27.9</u>	72.6	<u>72.1</u>	71.8
ToR-DAPO	39K (ViRL-39K)	54.3	31.6	74.2	73.0	73.6
<i>RLVR on Qwen-2.5-VL-3B</i>						
DAPO	2.1K (Geo3K)	42.25	22.6	64.0	57.8	54.7
ToR-DAPO	2.1K (Geo3K)	46.20	26.5	66.0	59.6	56.3
ToR-DAPO	39K (ViRL-39K)	47.50	28.3	67.5	62.4	60.8

5.1. Reasoning in Multi-modal LLMs

Existing approaches that focus on reasoning in multi-modal LLMs can be broadly categorized into:

- **Extending reasoning LLMs with visual understanding.** Building upon the strong reasoning capabilities of recent LLMs, one research branch explores incorporating visual content into LLMs. Typical strategies include: (1) integrating visual encoders into LLMs to directly extend them to multimodal scenarios (Peng et al., 2025; Wang et al., 2025b); and (2) transforming images into captions and feeding them into LLMs to bridge perception and reasoning (Huang et al., 2025; Wang et al., 2025e).

- **Enhancing reasoning abilities within MLLMs.** Another research branch seeks to endow existing MLLMs with reasoning skills. Representative approaches include: (1) transferring reasoning priors from reasoning LLMs into MLLMs through model merging, thereby leveraging the complementary strengths of both models (Chen et al., 2025b); and (2) adapting RLVR algorithms, such as Group Relative Policy Optimization (GRPO) (Shao et al., 2024), to enhance reasoning capabilities in multimodal settings (Huang et al.,

2025; Liu et al., 2025c; Li et al., 2026).

5.2. Reinforcement Learning with Verifiable Rewards

RLVR has recently demonstrated its effectiveness in aligning LLMs with verifiable reasoning outcomes. Among the implementations, GRPO (Shao et al., 2024) has shown great success with more stable advantage estimation. Subsequent refinements have further improved its efficiency and effectiveness (Yu et al., 2025b; Liu et al., 2025b; Wang et al., 2025c). When extending RLVR to multimodal settings, current methods primarily focus on two distinct branches:

- **Emphasizing the importance of visual understanding within RLVR.** Specifically, works like (Xiao et al., 2025; Yu et al., 2025a) introduce perception-oriented rewards to incentivize accurate visual grounding and understanding. Moreover, works such as (Liu et al., 2025a; Wang et al., 2025e; Li et al., 2025b) employ data augmentation strategies to improve model robustness and sensitivity against visual variations. Works like (Zhang et al., 2025c; Liu et al., 2025d) incorporate image manipulation tools like cropping and zooming in to focus on critical regions in the image during the reasoning process.

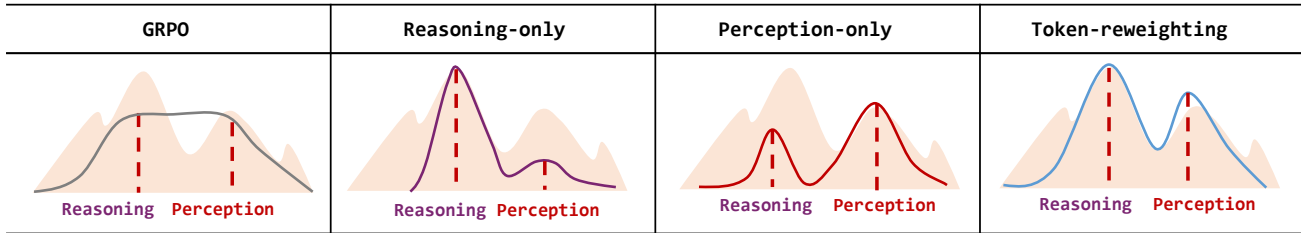


Figure 4. Comparison of optimization behaviors under different token selection strategies. Vanilla GRPO optimizes uniformly across all tokens. Reasoning-only and perception-only optimization concentrate on a single token type, leading to imbalanced training. Token reweighting jointly emphasizes reasoning- and perception-related tokens, achieving a more balanced optimization.

• **Constructing coherent reasoning chains with RLVR.** Representative works include: (1) distilling chain-of-thought reasoning patterns from stronger reasoning models to improve reasoning coherence in multimodal tasks (Huang et al., 2025; Wei et al., 2025); and (2) modifying different components of GRPO (e.g., clip ratios or advantage estimation) to emphasize reasoning-critical tokens better and stabilize training (Zhang et al., 2025b; Meng et al., 2025; Wang et al., 2025a).

Differences. Unlike existing methods that focus on optimizing either perception or reasoning abilities in isolation, our work systematically investigates and addresses the interdependence between these two capabilities. Specifically, through comprehensive token-level analysis, we demonstrate that perception and reasoning tokens exhibit complex interactions during training, where optimizing one type can inadvertently impair the other. To address this challenge, we propose a simple token-reweighting strategy that explicitly balances the optimization of both perception and reasoning tokens, leading to significant performance improvements across both capabilities.

6. Discussion

Understanding Token Reweighting. Unlike LLMs, MLLMs generate responses in which perception- and reasoning-related tokens are naturally interleaved. These tokens play different roles: perception-related tokens are responsible for grounding the visual inputs, while reasoning-related tokens determine key reasoning decisions. As illustrated in Figure 4, optimizing all tokens uniformly, as in vanilla GRPO, ignores this distinction and spreads learning signals over tokens that contribute little to reasoning or perception improvement.

Optimizing only reasoning-related tokens focuses on uncertain decision points and can improve reasoning quality, but it neglects perceptual tokens and weakens visual grounding. In contrast, optimizing only perception-related tokens strengthens visual grounding but leaves reasoning uncertainty largely unchanged, limiting reasoning capacities.

Token reweighting balances these two extremes by jointly emphasizing both reasoning- and perception-related tokens. This allows the model to improve critical reasoning decisions while still maintaining strong visual grounding, resulting in more stable and effective training across various backbones and data scales in practice.

7. Conclusion

In this work, through systematic token-wise analysis, we uncover a fundamental challenge in extending RLVR to multimodal LLMs: **the intrinsic interdependence between perception and reasoning**. We show that overemphasizing either capability inevitably impairs the other, yet current approaches overlook this issue and optimize them in isolation.

To address this, we proposed a simple yet effective **Token-Reweighting (ToR)** strategy that identifies and reweights perception- and reasoning-related tokens during RLVR training. We apply ToR over current RLVR algorithms (e.g., GRPO and DAPO), and achieve significant performance gains across diverse benchmarks, consistently enhancing both perception and reasoning.

Limitations and Future Work. While ToR establishes a foundation for addressing perception-reasoning interdependence, several promising directions remain open: ① **Fine-grained token identification strategies:** Precisely localizing critical regions in images using models like SAM (Kirillov et al., 2023) to identify more fine-grained perception-critical tokens. ② **Dynamic token reweighting:** Dynamically assigning weights to tokens based on their gradient contributions or connections to final outcomes (Yu et al., 2025c). ③ **Extending beyond tokens:** As tokens derive meaning from context, future work could explore perception-reasoning interdependence at broader contextual levels — optimizing tokens within their semantic context, preserving their contextual relationships. ④ **Exploring broader applications:** Extending this interdependence framework to more complex scenarios, e.g., unified multi-modal generation and understanding tasks (Wu et al., 2025; Deng et al., 2025a), where visual tokens participate in reasoning processes.

Impact Statements

This paper presents work whose goal is to advance the field of machine learning. There are many potential societal consequences of our work, none of which we feel must be specifically highlighted here.

References

- Bai, S., Chen, K., Liu, X., Wang, J., Ge, W., Song, S., Dang, K., Wang, P., Wang, S., Tang, J., et al. Qwen2. 5-vl technical report. *arXiv preprint arXiv:2502.13923*, 2025.
- Chen, H., Tu, H., Wang, F., Liu, H., Tang, X., Du, X., Zhou, Y., and Xie, C. SFT or RL? an early investigation into training rl-like reasoning large vision-language models. *Transactions on Machine Learning Research*, 2025a. ISSN 2835-8856. URL <https://openreview.net/forum?id=wZI5qkQeDF>.
- Chen, S., Zhang, J., Zhu, T., Liu, W., Gao, S., Xiong, M., Li, M., and He, J. Bring reason to vision: Understanding perception and reasoning through model merging. In *Forty-second International Conference on Machine Learning*, 2025b. URL <https://openreview.net/forum?id=ntCAP6tMoX>.
- Chen, Z., Wang, W., Cao, Y., Liu, Y., Gao, Z., Cui, E., Zhu, J., Ye, S., Tian, H., Liu, Z., et al. Expanding performance boundaries of open-source multimodal models with model, data, and test-time scaling. *arXiv preprint arXiv:2412.05271*, 2024.
- Cheng, D., Huang, S., Zhu, X., Dai, B., Zhao, W. X., Zhang, Z., and Wei, F. Reasoning with exploration: An entropy perspective. *arXiv preprint arXiv:2506.14758*, 2025.
- Deng, C., Zhu, D., Li, K., Gou, C., Li, F., Wang, Z., Zhong, S., Yu, W., Nie, X., Song, Z., et al. Emerging properties in unified multimodal pretraining. *arXiv preprint arXiv:2505.14683*, 2025a.
- Deng, Y., Bansal, H., Yin, F., Peng, N., Wang, W., and Chang, K.-W. OpenVLThinker: Complex vision-language reasoning via iterative SFT-RL cycles. In *The Thirty-ninth Annual Conference on Neural Information Processing Systems*, 2025b. URL <https://openreview.net/forum?id=gfXlnqBKtu>.
- Guan, T., Liu, F., Wu, X., Xian, R., Li, Z., Liu, X., Wang, X., Chen, L., Huang, F., Yacoob, Y., et al. Hallusionbench: an advanced diagnostic suite for entangled language hallucination and visual illusion in large vision-language models. In *Proceedings of the IEEE/CVF Conference on Computer Vision and Pattern Recognition*, pp. 14375–14385, 2024.
- Guo, D., Yang, D., Zhang, H., Song, J., Wang, P., Zhu, Q., Xu, R., Zhang, R., Ma, S., Bi, X., et al. Deepseek-r1 incentivizes reasoning in llms through reinforcement learning. *Nature*, 645(8081):633–638, 2025.
- Huang, W., Jia, B., Zhai, Z., Cao, S., Ye, Z., Zhao, F., Xu, Z., Hu, Y., and Lin, S. Vision-r1: Incentivizing reasoning capability in multimodal large language models. *arXiv preprint arXiv:2503.06749*, 2025.
- Kirillov, A., Mintun, E., Ravi, N., Mao, H., Rolland, C., Gustafson, L., Xiao, T., Whitehead, S., Berg, A. C., Lo, W.-Y., et al. Segment anything. In *Proceedings of the IEEE/CVF international conference on computer vision*, pp. 4015–4026, 2023.
- Lambert, N., Morrison, J., Pyatkin, V., Huang, S., Ivison, H., Brahman, F., Miranda, L. J. V., Liu, A., Dziri, N., Lyu, X., Gu, Y., Malik, S., Graf, V., Hwang, J. D., Yang, J., Bras, R. L., Taffjord, O., Wilhelm, C., Soldaini, L., Smith, N. A., Wang, Y., Dasigi, P., and Hajishirzi, H. Tulu 3: Pushing frontiers in open language model post-training. In *Second Conference on Language Modeling*, 2025. URL <https://openreview.net/forum?id=iluGbfHHpH>.
- Li, B., Zhang, Y., Guo, D., Zhang, R., Li, F., Zhang, H., Zhang, K., Zhang, P., Li, Y., Liu, Z., and Li, C. LLaVA-onevision: Easy visual task transfer. *Transactions on Machine Learning Research*, 2025a. ISSN 2835-8856. URL <https://openreview.net/forum?id=zKv8qULV6n>.
- Li, J., Fang, J., Lu, J., Wang, Y., Guo, X., Zhang, T., Wang, X., and He, X. Enhancing multi-modal llms reasoning via difficulty-aware group normalization, 2026. URL <https://arxiv.org/abs/2602.21743>.
- Li, Y., Wei, L., Zheng, K., Huang, J., Kong, L., Sun, L., and Huang, W. Vision matters: Simple visual perturbations can boost multimodal math reasoning. *arXiv preprint arXiv:2506.09736*, 2025b.
- Liu, X., Ni, J., Wu, Z., Du, C., Dou, L., Wang, H., Pang, T., and Shieh, M. Q. Noisyrollout: Reinforcing visual reasoning with data augmentation. In *2nd AI for Math Workshop @ ICML 2025*, 2025a. URL <https://openreview.net/forum?id=GdNm9PEAei>.
- Liu, Z., Chen, C., Li, W., Qi, P., Pang, T., Du, C., Lee, W. S., and Lin, M. Understanding rl-zero-like training: A critical perspective. In *2nd AI for Math Workshop @ ICML 2025*, 2025b. URL <https://openreview.net/forum?id=jLpC1zavzn>.
- Liu, Z., Sun, Z., Zang, Y., Dong, X., Cao, Y., Duan, H., Lin, D., and Wang, J. Visual-rft: Visual reinforcement fine-tuning. In *Proceedings of the IEEE/CVF International*

- Conference on Computer Vision (ICCV)*, pp. 2034–2044, October 2025c.
- Liu, Z., Zang, Y., Zou, Y., Liang, Z., Dong, X., Cao, Y., Duan, H., Lin, D., and Wang, J. Visual agentic reinforcement fine-tuning. *arXiv preprint arXiv:2505.14246*, 2025d.
- Lu, J., Wang, S., Zhang, X., Hao, Y., and He, X. Semantic-based selection, synthesis, and supervision for few-shot learning. In *Proceedings of the 31st ACM International Conference on Multimedia*, pp. 3569–3578, 2023.
- Lu, J., Wang, S., Hao, Y., Liu, H., Wang, X., and Wang, M. Rethinking visual content refinement in low-shot clip adaptation. *arXiv preprint arXiv:2407.14117*, 2024a.
- Lu, J., Li, J., Gao, Y., Wu, J., Wu, J., Wang, X., and He, X. Adavip: Aligning multi-modal llms via adaptive vision-enhanced preference optimization, 2025a. URL <https://arxiv.org/abs/2504.15619>.
- Lu, J., Wu, J., Li, J., Jia, X., Wang, S., Zhang, Y., Fang, J., Wang, X., and He, X. Dama: Data-and model-aware alignment of multi-modal llms. In *International Conference on Machine Learning*, pp. 40726–40740. PMLR, 2025b.
- Lu, P., Gong, R., Jiang, S., Qiu, L., Huang, S., Liang, X., and Zhu, S.-c. Inter-gps: Interpretable geometry problem solving with formal language and symbolic reasoning. In *Proceedings of the 59th Annual Meeting of the Association for Computational Linguistics and the 11th International Joint Conference on Natural Language Processing (Volume 1: Long Papers)*, pp. 6774–6786, 2021.
- Lu, P., Bansal, H., Xia, T., Liu, J., Li, C., Hajishirzi, H., Cheng, H., Chang, K.-W., Galley, M., and Gao, J. Mathvista: Evaluating mathematical reasoning of foundation models in visual contexts. In *The Twelfth International Conference on Learning Representations*, 2024b. URL <https://openreview.net/forum?id=KUNzEQMWU7>.
- Meng, F., Du, L., Liu, Z., Zhou, Z., Lu, Q., Fu, D., Shi, B., Wang, W., He, J., Zhang, K., et al. Mm-eureka: Exploring visual aha moment with rule-based large-scale reinforcement learning. *CoRR*, 2025.
- Peng, Y., Wang, P., Wang, X., Wei, Y., Pei, J., Qiu, W., Jian, A., Hao, Y., Pan, J., Xie, T., et al. Skywork r1v: Pioneering multimodal reasoning with chain-of-thought. *arXiv preprint arXiv:2504.05599*, 2025.
- Qiao, R., Tan, Q., Dong, G., Wu, M., Sun, C., Song, X., GongQue, Z., Lei, S., Wei, Z., Zhang, M., et al. We-math: Does your large multimodal model achieve human-like mathematical reasoning? *arXiv preprint arXiv:2407.01284*, 2024.
- Shao, Z., Wang, P., Zhu, Q., Xu, R., Song, J., Bi, X., Zhang, H., Zhang, M., Li, Y., Wu, Y., et al. Deepseekmath: Pushing the limits of mathematical reasoning in open language models. *arXiv preprint arXiv:2402.03300*, 2024.
- Wang, H., Qu, C., Huang, Z., Chu, W., Lin, F., and Chen, W. VL-rethinker: Incentivizing self-reflection of vision-language models with reinforcement learning. In *The Thirty-ninth Annual Conference on Neural Information Processing Systems*, 2025a. URL <https://openreview.net/forum?id=4oYxzssbVg>.
- Wang, K., Pan, J., Shi, W., Lu, Z., Ren, H., Zhou, A., Zhan, M., and Li, H. Measuring multimodal mathematical reasoning with math-vision dataset. *Advances in Neural Information Processing Systems*, 37:95095–95169, 2024.
- Wang, P., Wei, Y., Peng, Y., Wang, X., Qiu, W., Shen, W., Xie, T., Pei, J., Zhang, J., Hao, Y., et al. Skywork r1v2: Multimodal hybrid reinforcement learning for reasoning. *arXiv preprint arXiv:2504.16656*, 2025b.
- Wang, S., Yu, L., Gao, C., Zheng, C., Liu, S., Lu, R., Dang, K., Chen, X.-H., Yang, J., Zhang, Z., Liu, Y., Yang, A., Zhao, A., Yue, Y., Song, S., Yu, B., Huang, G., and Lin, J. Beyond the 80/20 rule: High-entropy minority tokens drive effective reinforcement learning for LLM reasoning. In *The Thirty-ninth Annual Conference on Neural Information Processing Systems*, 2025c. URL <https://openreview.net/forum?id=yfcpdY4gMP>.
- Wang, X., Yang, Z., Feng, C., Lu, H., Li, L., Lin, C.-C., Lin, K., Huang, F., and Wang, L. SoTA with less: MCTS-guided sample selection for data-efficient visual reasoning self-improvement. In *The Thirty-ninth Annual Conference on Neural Information Processing Systems*, 2025d. URL <https://openreview.net/forum?id=PHu9xJeAum>.
- Wang, Z., Guo, X., Stoica, S., Xu, H., Wang, H., Ha, H., Chen, X., Chen, Y., Yan, M., Huang, F., et al. Perception-aware policy optimization for multimodal reasoning. *arXiv preprint arXiv:2507.06448*, 2025e.
- Wei, L., Li, Y., Zheng, K., Wang, C., Wang, Y., Kong, L., Sun, L., and Huang, W. Advancing multimodal reasoning via reinforcement learning with cold start. *arXiv preprint arXiv:2505.22334*, 2025.
- Wu, C., Li, J., Zhou, J., Lin, J., Gao, K., Yan, K., Yin, S.-m., Bai, S., Xu, X., Chen, Y., et al. Qwen-image technical report. *arXiv preprint arXiv:2508.02324*, 2025.
- Xiao, T., Xu, X., Huang, Z., Gao, H., Liu, Q., Liu, Q., and Chen, E. Advancing multimodal reasoning capabilities of multimodal large language models via visual perception reward. *arXiv preprint arXiv:2506.07218*, 2025.

- Yang, A., Li, A., Yang, B., Zhang, B., Hui, B., Zheng, B., Yu, B., Gao, C., Huang, C., Lv, C., et al. Qwen3 technical report. *arXiv preprint arXiv:2505.09388*, 2025a.
- Yang, Y., He, X., Pan, H., Jiang, X., Deng, Y., Yang, X., Lu, H., Yin, D., Rao, F., Zhu, M., Zhang, B., and Chen, W. R1-onevision: Advancing generalized multimodal reasoning through cross-modal formalization. In *Proceedings of the IEEE/CVF International Conference on Computer Vision (ICCV)*, pp. 2376–2385, October 2025b.
- Yaowei, Z., Junting, L., Shenzhi, W., Zhangchi, F., Dongdong, K., and Yuwen, X. Easyr1: An efficient, scalable, multi-modality rl training framework. <https://github.com/hiyouga/EasyR1>, 2025.
- Yu, E., Lin, K., Zhao, L., jisheng yin, Wei, Y., Peng, Y., Wei, H., Sun, J., Han, C., Ge, Z., Zhang, X., Jiang, D., Wang, J., and Tao, W. Perception-r1: Pioneering perception policy with reinforcement learning. In *The Thirty-ninth Annual Conference on Neural Information Processing Systems*, 2025a. URL <https://openreview.net/forum?id=BeXcXrXetA>.
- Yu, Q., Zhang, Z., Zhu, R., Yuan, Y., Zuo, X., Yue, Y., Dai, W., Fan, T., Liu, G., Liu, L., et al. Dapo: An open-source llm reinforcement learning system at scale. *arXiv preprint arXiv:2503.14476*, 2025b.
- Yu, T., Ji, B., Wang, S., Yao, S., Wang, Z., Cui, G., Yuan, L., Ding, N., Yao, Y., Liu, Z., et al. Rlpr: Extrapolating rlvr to general domains without verifiers. *arXiv preprint arXiv:2506.18254*, 2025c.
- Zhang, J., Huang, J., Yao, H., Liu, S., Zhang, X., Lu, S., and Tao, D. R1-vl: Learning to reason with multimodal large language models via step-wise group relative policy optimization. In *Proceedings of the IEEE/CVF International Conference on Computer Vision (ICCV)*, pp. 1859–1869, October 2025a.
- Zhang, R., Jiang, D., Zhang, Y., Lin, H., Guo, Z., Qiu, P., Zhou, A., Lu, P., Chang, K.-W., Qiao, Y., et al. Mathverse: Does your multi-modal llm truly see the diagrams in visual math problems? In *European Conference on Computer Vision*, pp. 169–186. Springer, 2024.
- Zhang, Y.-F., Lu, X., Hu, X., Fu, C., Wen, B., Zhang, T., Liu, C., Jiang, K., Chen, K., Tang, K., et al. R1-reward: Training multimodal reward model through stable reinforcement learning. *arXiv preprint arXiv:2505.02835*, 2025b.
- Zhang, Y.-F., Lu, X., Yin, S., Fu, C., Chen, W., Hu, X., Wen, B., Jiang, K., Liu, C., Zhang, T., et al. Thyme: Think beyond images. *arXiv preprint arXiv:2508.11630*, 2025c.
- Zhu, J., Wang, W., Chen, Z., Liu, Z., Ye, S., Gu, L., Tian, H., Duan, Y., Su, W., Shao, J., et al. Internvl3: Exploring advanced training and test-time recipes for open-source multimodal models. *arXiv preprint arXiv:2504.10479*, 2025.

A. Token Distribution and Characteristic Analysis

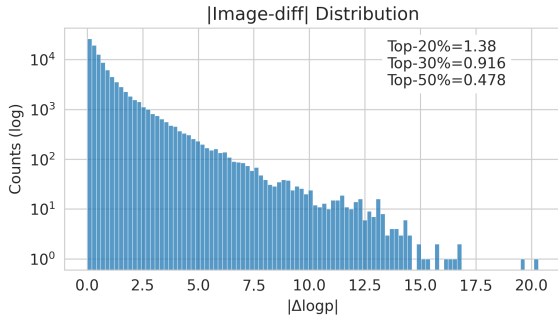


Figure 5. Distribution of log-probability differences for Qwen-2.5-VL-7B on HallusionBench, used to identify perception-related tokens (Guan et al., 2024).

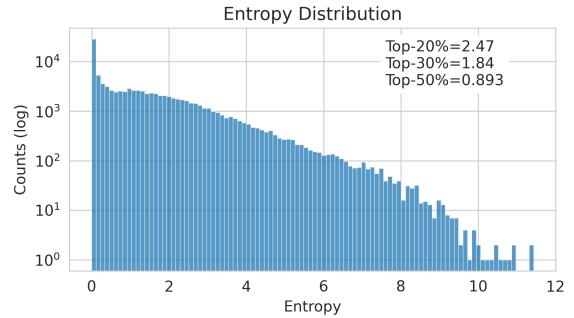


Figure 6. Distribution of entropy values for Qwen-2.5-VL-7B on HallusionBench, used to identify reasoning-related tokens (Guan et al., 2024).

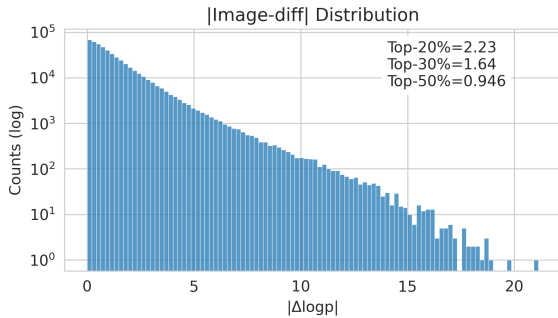


Figure 7. Distribution of log-probability differences for Qwen-2.5-VL-7B on WeMath, used to identify perception-related tokens (Qiao et al., 2024).

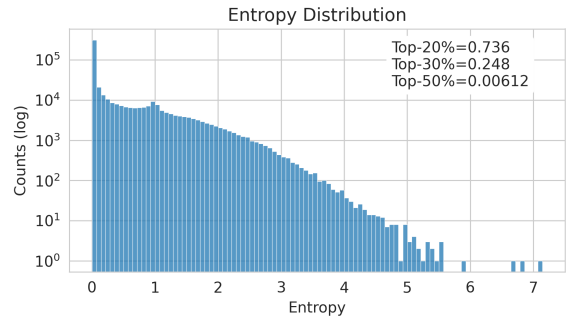


Figure 8. Distribution of entropy values for Qwen-2.5-VL-7B on WeMath, used to identify reasoning-related tokens (Qiao et al., 2024).

To further investigate the characteristics of perception- and reasoning-related tokens, we analyze the token distribution of Qwen-2.5-VL-7B on both perception and reasoning benchmarks. Specifically, we report the entropy distribution (Figures 6, 8) and the image log-probability difference distribution (Figures 5, 7) on *HallusionBench* (Guan et al., 2024) and *WeMath* (Qiao et al., 2024), respectively. For each case, we further highlight the values corresponding to the top 20%, 30%, and 50% of tokens, ranked by their entropy or log-probability differences.

Our observations are as follows:

① Perception-related benchmark (Guan et al., 2024). High-entropy tokens exhibit large variations, with more than 50% of tokens exceeding 0.89. In contrast, the image log-probability difference of perception-related tokens is relatively stable: more than 70% of tokens are less than 0.916. This indicates that a small set of perception-related tokens is consistently stable and plays a critical role in capturing visual cues, suggesting that focusing on these tokens effectively enhances the model’s perceptual ability.

② Reasoning-related benchmark (Qiao et al., 2024). In reasoning tasks, the distribution shows the opposite trend. Perception-related tokens present large variations, with more than 50% exceeding 0.946. Meanwhile, high-entropy tokens remain relatively stable, with over 70% less than 0.248. This implies that a small subset of reasoning-related tokens is more robust and can effectively capture the key reasoning process, highlighting their importance in enhancing the model’s reasoning capability.

These results demonstrate that perception and reasoning rely on different types of stable tokens: perception emphasizes stability in a small number of visually sensitive tokens, while reasoning relies on the robustness of high-entropy tokens. This contrast validates our token re-weighting strategy that explicitly leverages both perception- and reasoning-related tokens.

B. Perception-Reasoning Interdependence

In this section, we demonstrate the interdependence between perception and reasoning tokens. Specifically, we visualize the relationship between reasoning uncertainty and perception strength over the training and validation set of Geo3K (Figure 9 & Figure 10), where we can observe a strong push-pull dynamic relationship between the reasoning and perception.

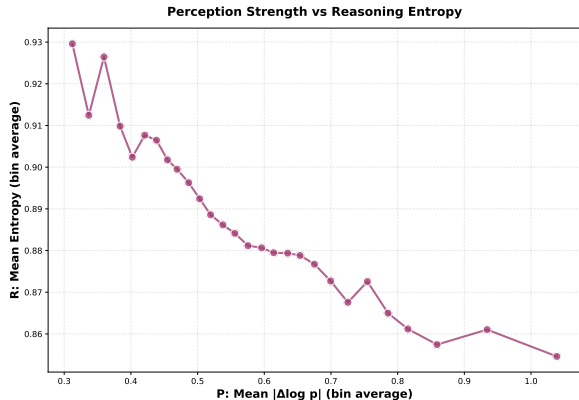


Figure 9. Relationship between (1) reasoning uncertainty: the entropy value of reasoning tokens and (2) perceptron strength: the logp diff between perception tokens for each response over Geo3K training set, response sampled from Qwen-2.5-VL 7B.

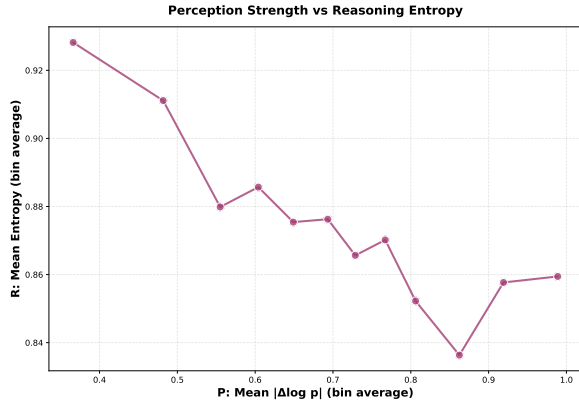


Figure 10. Relationship between (1) reasoning uncertainty: the entropy value of reasoning tokens and (2) perceptron strength: the logp diff between perception tokens for each response over Geo3K validation set, response sampled from Qwen-2.5-VL 7B.

C. Perception Token Identification with Various Criteria

Identifying perception-related tokens is a key component of Token Reweighting. Since perception relevance is not directly observable, we investigate several feasible proxy criteria derived from the model’s predicted distributions. Specifically, we compare the following four alternatives: *probability difference* (prob-diff), *log-probability difference* (logp-diff), *entropy difference* (entropy-diff), and *attention scores* to image features.

Proxy criteria. Given a generated token o_t , conditioned on either the image I or an empty image placeholder \emptyset , we consider: (i) prob-diff, measuring absolute probability change; (ii) logp-diff, measuring relative probability change; (iii) entropy-diff, measuring distribution-level uncertainty change; and (iv) attention scores, which directly reflect visual grounding but are computationally expensive to store during rollout and thus used only for analysis.

Visual grounding fidelity. We first evaluate how well each proxy captures visual grounding by measuring its rank correlation with attention scores to image tokens. Results on Geo3K, WeMath, and HallusionBench are reported in Figure 11 → Figure 19. Among all probability-based proxies, *prob-diff* exhibits the strongest correlation with attention scores, indicating that it best reflects the *absolute influence* of the image on individual token predictions. In contrast, entropy-diff shows the weakest correlation, as it measures global distribution changes rather than token-level visual dependence.

Information-theoretic significance. While prob-diff captures visual influence effectively, it treats equal-magnitude probability changes as equally important, regardless of their relative scale. Entropy-diff, on the other hand, directly measures changes in model uncertainty and is information-theoretically well grounded, but lacks token-level localization. These observations reveal a fundamental trade-off between accurately capturing *how much the image matters* and *how meaningful the change is*.

Log-probability difference as a balanced proxy. Logp-diff naturally balances these two aspects. Empirically, it achieves rank correlations with attention scores close to those of prob-diff, while simultaneously accounting for the relative significance of probability changes. This makes logp-diff more sensitive to informative but low-probability tokens, which are common in multimodal reasoning. As a result, logp-diff provides a more faithful token-level estimate of visual relevance.

Impact on training performance. Table 5 reports downstream performance when different proxies are used within the ToR framework. Across HallusionBench, WeMath, and MathVerse, logp-diff consistently yields the largest gains over the GRPO baseline, outperforming both prob-diff and entropy-diff. This empirical advantage aligns with the above analysis,

Table 5. Comparison of different perception proxies within the ToR framework. Performance is reported on HallusionBench, WeMath, and MathVerse. Gains are computed relative to the GRPO baseline.

Perception Proxy	HallusionBench	WeMath	MathVerse	Avg. Gain
Baseline (GRPO)	69.8	67.4	50.8	–
Prob Diff (best visual grounding)	71.8 (+2.0)	68.5 (+1.1)	52.6 (+1.8)	+1.6%
Entropy Diff (best info-theoretic)	70.9 (+1.1)	67.9 (+0.5)	51.5 (+0.7)	+0.8%
Logp Diff (best balance)	72.4 (+2.6)	68.9 (+1.5)	53.0 (+2.2)	+2.1%

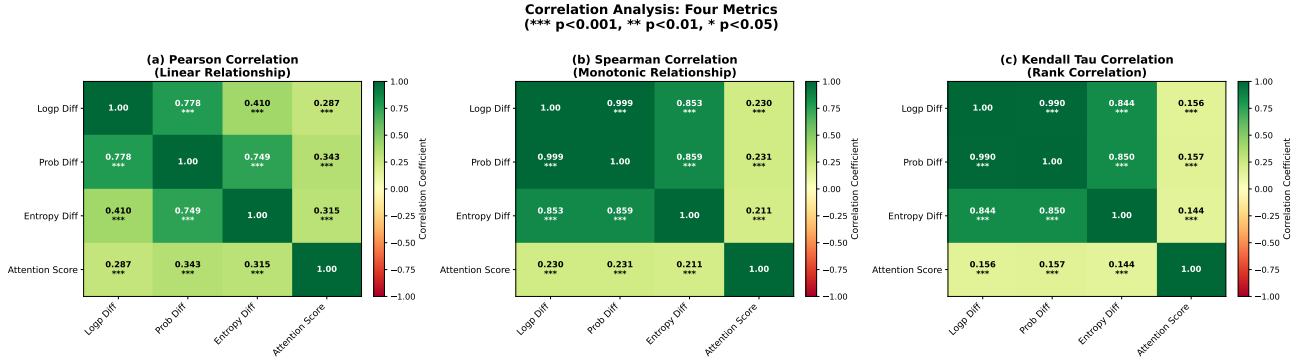


Figure 11. Correlation heatmaps between different image token selection strategies over the validation set.

suggesting that balancing visual grounding fidelity and information-theoretic significance is critical for effective perception token identification.

Summary. Overall, prob-diff excels at capturing absolute visual influence but lacks information-theoretic sensitivity, while entropy-diff is theoretically principled yet poorly localized. Logp-diff offers a balanced alternative, preserving strong visual grounding signals while properly weighting the significance of probability changes. This balance makes logp-diff the most effective and robust proxy for identifying perception-related tokens in Token Reweighting.

D. Distribution of Selected Tokens over Various Rollouts.

In this section, we show the distribution of selected tokens over a batch of rollouts as in Figure 20. We can find that different rollouts receive a comparable overall amount of optimization, but with different mixtures of tokens: harder groups are optimized more on reasoning, easier groups more on perception, while both token types remain well represented across the rollout batch.

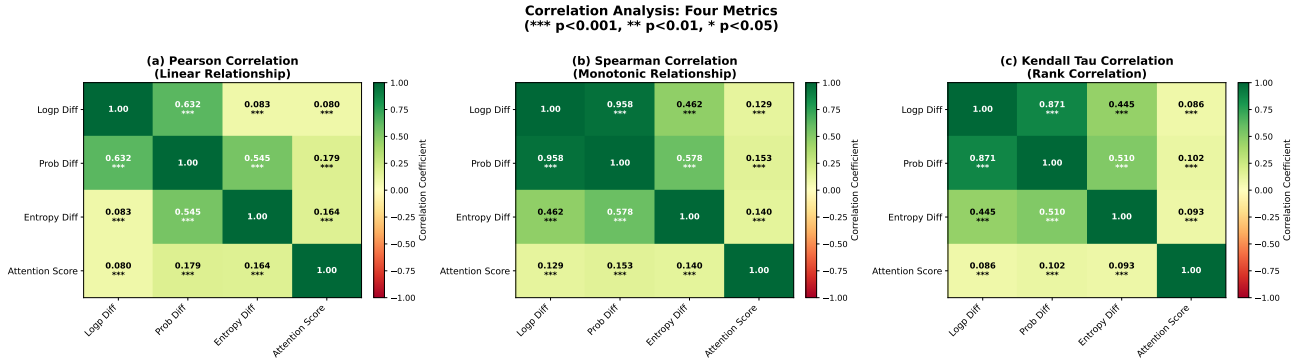


Figure 12. Correlation heatmaps between different image token selection strategies over the hallubench benchmark.

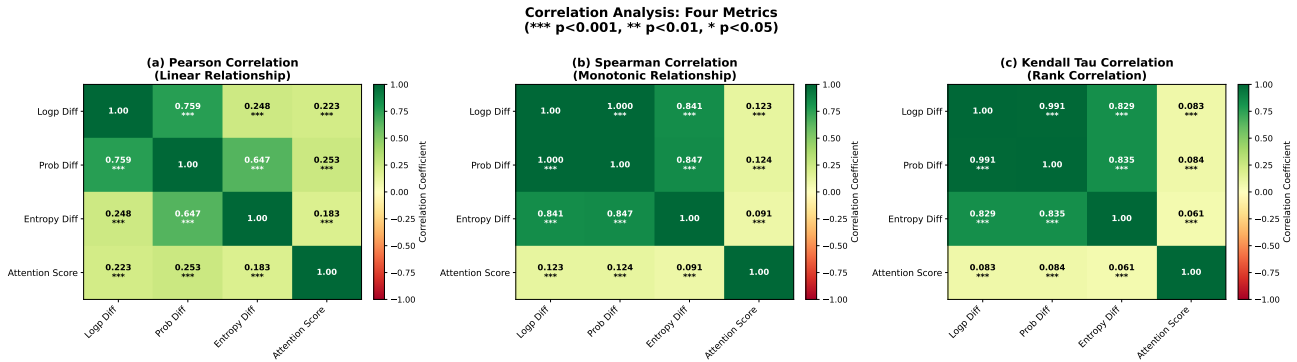


Figure 13. Correlation heatmaps between different image token selection strategies over the wemath benchmark.

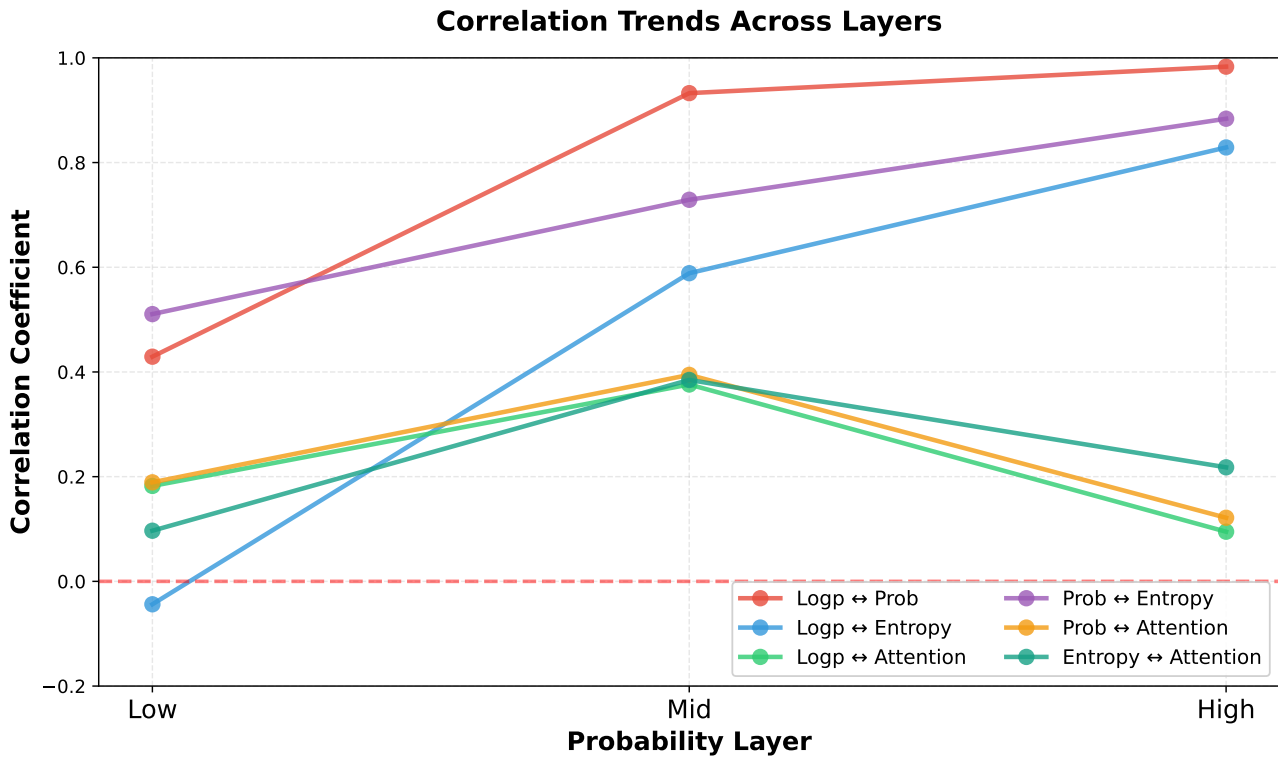


Figure 14. Correlation comparison across layers between different image token selection strategies over the validation set.

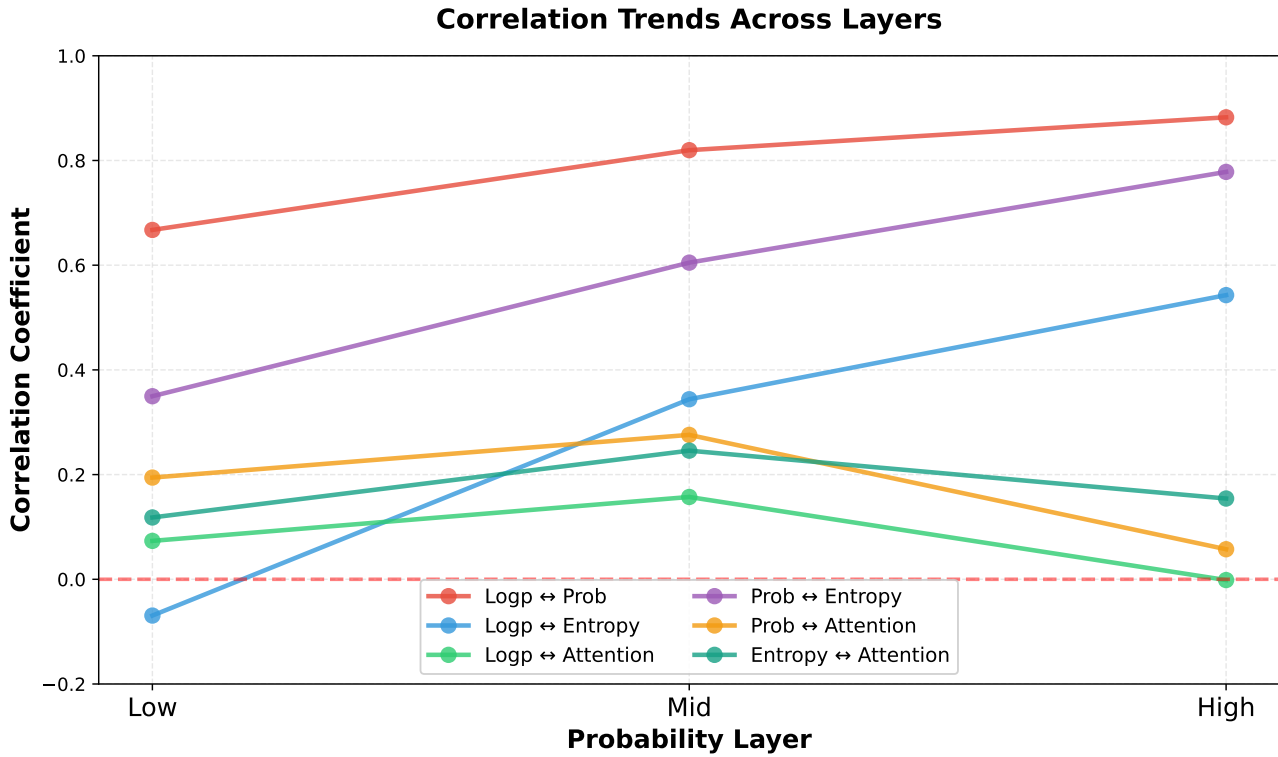


Figure 15. Correlation comparison across layers between different image token selection strategies over the hallubench benchmark.

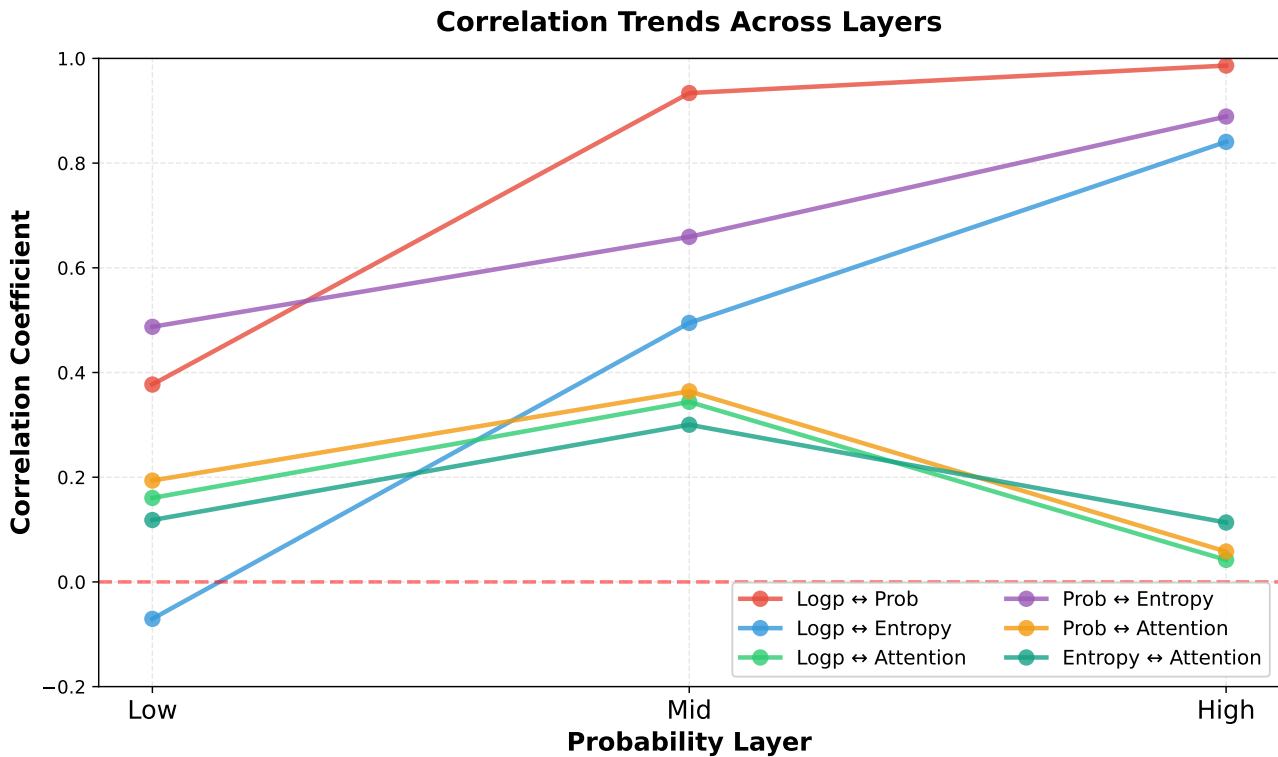


Figure 16. Correlation comparison across layers between different image token selection strategies over the wemath benchmark.

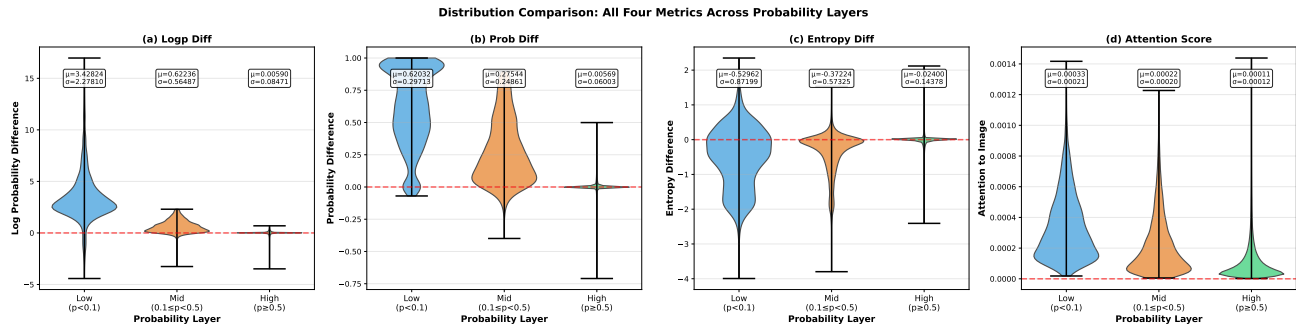


Figure 17. violin plot between different image token selection strategies over the validation set.

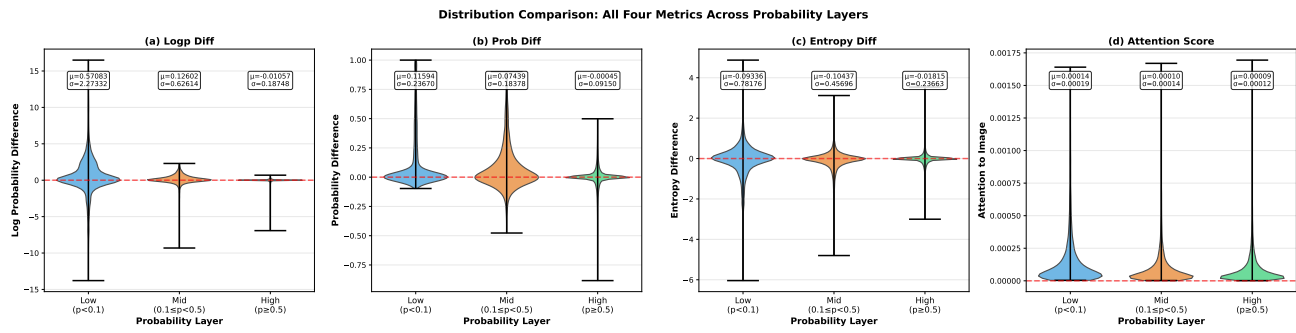


Figure 18. violin plot between different image token selection strategies over the Hallubench benchmark.

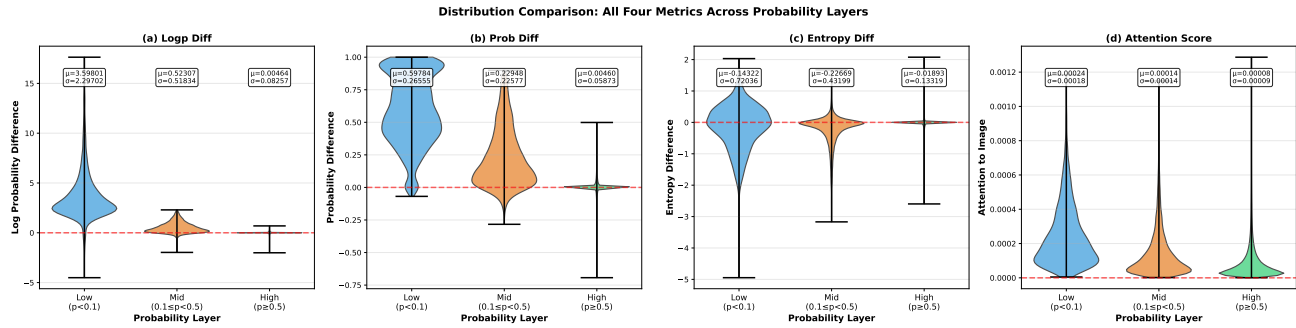


Figure 19. violin plot between different image token selection strategies over the wemath benchmark.

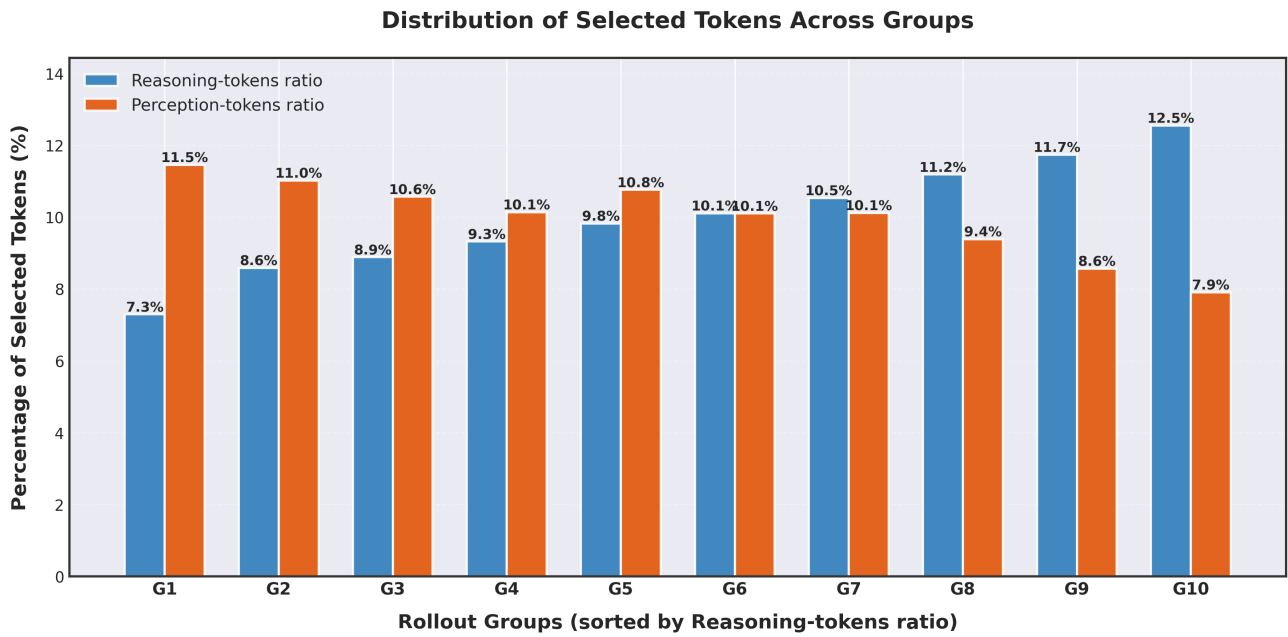


Figure 20. Distribution of selected tokens over the sampled rollouts, where we employ the Qwen-VL-2.5 7B model with a batch of 512 samples, each sample generates 16 rollout responses.